

# Application of electromagnetic techniques to subsurface exploration

Author: Imma Gonzalez Prats

*Facultat de Física, Universitat de Barcelona, Diagonal 645, 08028 Barcelona, Spain.*

Advisor: Alejandro Marcuello Pascual, alex.marcuello@ub.edu

**Abstract:** This work explores in depth the basis of the electrodynamic induction method and uses it to characterize the electrical conductivity of the ground in a contaminated area near Òdena (Catalunya, Spain). This work aims to evaluate the viability of this method. The process involves collecting and analysing apparent conductivity data using CMD Mini Explorer, inverting them using EMagPy software, and plotting them using Surfer. By comparing different measurements with the available studies of the area, it is possible to characterize it and reliably identify the anomalies and their trends.

**Keywords:** electrical conductivity, electromagnetic induction methods, soil contamination

**SDGs:** good health and well-being (3), clean water and sanitation (6), life on land (15), partnerships for the goals (17)

## I. INTRODUCTION

The diagnosis and remediation of organochlorine (DNAPL) contamination in soils and groundwater is a significant challenge for the scientific community due to the propensity of these compounds to migrate from the unsaturated zone (ZNS) to aquifers. The complexity of this problem increases when the aquifer is fractured, due to its heterogeneity. The exploration of these hydrogeological units helps to understand the trajectories and the residence times of these components in the soil. Different techniques are usually employed to achieve a complete and detailed characterization. It is a widespread and highly relevant problem in European groundwater because it can pose a danger to human health (J. Luque Marín, personal communication: email, 15th April 2025).

An example of this problem is the contaminated area of Òdena (Catalunya, Spain), where an unconfined fractured bedrock aquifer is present. The contamination came from an old chemical dye factory that operated between 1978 and 1985. When the factory closed, the contaminant sources remained until they were removed in 2005, but some organochlorines had already percolated into the subsoil. The three main sources of contamination were an underground wastewater tank, a disposal lagoon and abandoned solvent barrels inside the building [1]. Multiple studies and remediation campaigns were carried out between 2014 and 2024, during which piezometric levels, electrical tomography, pumping and slug tests, physicochemical parameters, and major cations and anions were recorded.

The aim of this work is to evaluate the viability of the electromagnetic induction method by characterizing a contaminated area and comparing the results with other characterization methods. The electromagnetic induction method is based on evaluating the soil properties by emitting a magnetic field to induce eddy currents and measuring a combination of the primary

and secondary magnetic fields, the latter resulting from subsurface response. The technique is non-invasive and cost-effective, though with limited depth resolution [2].

## II. PHYSICS FOUNDATIONS

### A. Electromagnetic induction method

The electromagnetic induction method is based on the Faraday-Lenz law, which states that an electric field is induced in presence of a variable magnetic flux.

The application process is as follows: the measuring device contains a transmitting coil that, through an alternating current, generates a primary variable magnetic field ( $H_p$ ). This field interacts with the conductive soil, thereby inducing electrical currents and creating a secondary magnetic field ( $H_s$ ). The receiving coil records the superposition of primary and secondary magnetic fields. By analysing the relationship between these fields, one can deduce the apparent conductivity of the subsoil, which also depends on the position of the coils and the operating frequency [3].

The expressions for primary and secondary magnetic fields can be derived from Maxwell's equations and under the assumptions of harmonic current, magnetic inhomogeneities, a single layer and low frequency. The relationship between these fields depends on the orientation of the magnetic dipole, with distinct expressions for vertical (1) and horizontal (2) dipole as follows:

$$\frac{H^s}{H^p} = \frac{2}{\gamma^2 \rho^2} [9 - (9\gamma\rho + 4\gamma^2\rho^2 + \gamma^3\rho^3)e^{-\gamma\rho}], \quad (1)$$

$$\frac{H^s}{H^p} = \frac{2}{\gamma^2 \rho^2} [-3 + \gamma\rho + \gamma^2\rho^2 + (3 + 3\gamma\rho + \gamma^2\rho^2)e^{-\gamma\rho}], \quad (2)$$

where  $\gamma = \sqrt{i2\pi f\mu_0\sigma}$ , being  $\mu_0$  the vacuum permeability,  $f$  the frequency,  $\sigma$  the conductivity and  $\rho$  the coils distance.

These expressions are called McNeill's equations, and can be rewritten introducing the induction number  $B = \frac{\gamma\rho}{\sqrt{2i}}$  (related to the magnetic field attenuation [3]). Since using the parameters of the measurement instrument of this work the value of  $B \leq 10^{-1}$ , taking only the imaginary part and performing Taylor expansion, we get:

$$\frac{H^s}{H^p} = i \left[ \frac{B^2}{2} - \frac{8B^3}{15} + \mathcal{O}(B^3) \right], \quad (3)$$

$$\frac{H^s}{H^p} = i \left[ \frac{B^2}{2} - \frac{4B^3}{15} + \mathcal{O}(B^3) \right]. \quad (4)$$

For very small B in both cases:

$$\frac{H^s}{H^p} = \frac{2\pi f i \mu_0 \sigma \rho^2}{4}. \quad (5)$$

This is the expression that gives a relation between the apparent conductivity and the ratio of the fields, linear for low induction numbers. The real part, n-phase component, is not relevant to this analysis because its contributions come from ground magnetic susceptibility and also the relation with the conductivity is not linear [4].

The differences in the relations between the field cause variations in the sensitivity. Figure 1 illustrates the sensitivity functions of few meters depth.

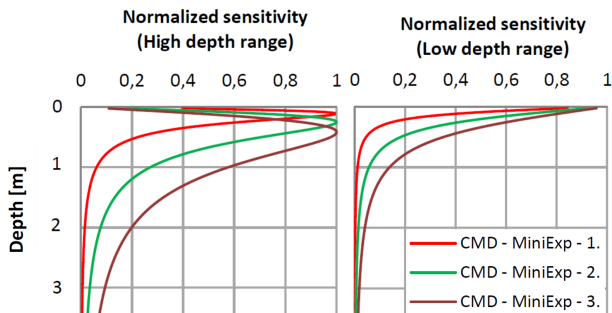


Figure 1: Sensitivity functions for High and Low depth range for CMD Mini Explorer at coil distances C1, C2 and C3 [2].

$D/\rho = 1/\sqrt{8}$ , therefore the maximum sensibility is at the depth of  $0.35\rho$ . In the horizontal mode, the maximum of the function is when  $D/\rho = 0$ , therefore the maximum sensibility is at the surface [4].

### B. Inversion method

Geophysical inversion is a methodology to obtain subsurface models by finding a model where the distribution of physical properties explains the observed measurements.

The first step of this process is parametrization and the definition of the system constraints, considering

any known information or other data from our area. With this initial model, forward modeling is applied to simulate the expected data, which is then compared with the real data. The difference between the two data sets is reduced by adjusting parameters through iterative optimization techniques until the result is similar enough [5]. Since it is a non-unique problem, initial parameters and constraints must be chosen carefully.

For the inversion of frequency-domain electromagnetic data I have considered the EMagPy program [6], which retrieves electrical conductivity models of the subsurface through 1D inversion. It treats each measurement point as an independent vertical sounding, assuming a horizontally layered earth model, and estimates the conductivities and depths accordingly. A wide variety of minimization methods, both in the linear approximation and using the full solution of Maxwell's equations, can be used [5]. The Root Mean Square Percentage Error (RMSPE) evaluates the fitting quality by measuring the relative accuracy between real and model data. An accurate model is characterized by a low RMSPE value [3]. Its expression is:

$$RMSPE = 100 \cdot \sqrt{\frac{1}{n} \sum_{i=1}^n \left( \frac{d_i - r_i}{d_i} \right)^2}, \quad (6)$$

being  $n$  the number of data,  $d_i$  the real data and  $r_i$  the modelled data.

## III. EXPERIMENTAL PROCEDURE

### A. Field Work

Data were collected with an electromagnetic conductivity meter, the CMD Mini Explorer from GF Instruments [7], which consists of a coil assembly in a tube and the control unit. Measurements can be taken continuously, with a set time interval, or discretely, where the operator selects the measurement points. A GPS device can be attached to georeference the data. Additionally, coil position can be adjusted: the vertical coil orientation (horizontal dipole) is called Low mode, and the horizontal coil orientation (vertical dipole) is called High mode, affecting sensitivity and penetration depth of the measurements. All measurements were performed at three different coil separations (C1=0.32 m, C2=0.71 m and C3=1.18 m) corresponding to three depths, as the instrument is equipped with three receiver coils. The operating frequency is 30 kHz [2].

Data acquisition was conducted using two different methods: profiles and maps. Mapping 1 was conducted in the field adjacent to the factory and Mapping 2, in the neighbouring. Both profiles were acquired in the first field, perpendicular to each other. Profile 1, the longer one, is oriented S-N and 131 m long (262 data points),

while Profile 2, the shorter one, is oriented NW-SE and 39.5 m long (79 data points). All locations (Fig. 2) were selected based on known contamination sources and prior studies.

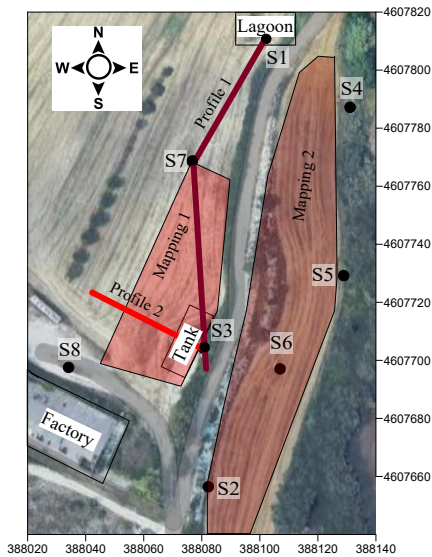


Figure 2: Overview of the study area showing surveyed profiles and mappings (Google @2025Airbus, Google Earth [8]).

Maps were conducted using GPS-based continuous location, while profiles were performed manually, taking measurements every half meter. Near the factory, both coil modes (Low and High) were used, whereas in the neighbouring field, only the High mode was employed.

## B. Data

Data files are stored as binary files in CMD Mini Explorer. Using the CMD Data Transfer program, these files are converted into .txt and .dat files with UTM coordinates.

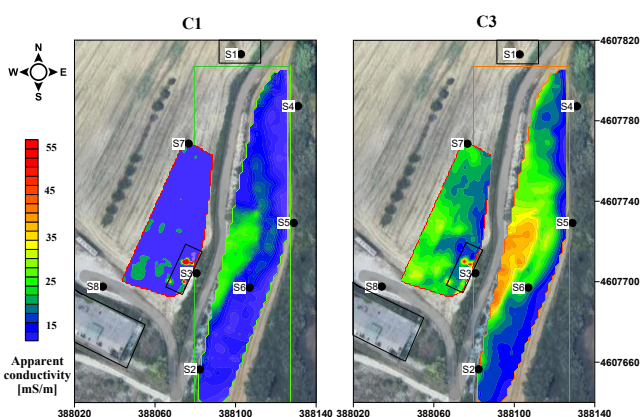


Figure 3: Data mappings (C1 and C3) in High mode (Google @2025Airbus, Google Earth) [6][8].

The first file contains information about the measurements (metadata), and the second one contains the data. The interesting data for this project are the coordinates [UTM], the apparent conductivities [mS/m], and the in-phase [parts per thousand, ppt] [2]. This data must be saved in a .csv file to proceed with the inversion using the EMagPy program. In this program, a starting model must be set before performing the inversion.

Based on previous lithological studies and trial-and-error tests, a two-layer model with a 1 m thick superficial layer was considered. The EMagPy program provides inverted conductivities and graphical profiles representation. The Surfer program was used for the real (Fig. 3) and inverted mapping data representation.

## C. Results

Data processing provided the inverted maps. Focusing on Mapping 1, which is significant due to its proximity to ancient contaminant sources, results from both modes are compared (Fig. 4, left). Only C1 and C3 are represented to show the maximum contrast, being C1 the shallowest depth. Conductivity values range between 5 and 105 mS/m, increasing with depth. Small conductivity anomalies corresponding to metal boxes installed for other studies are identified, especially around S3. This comparison is valuable as the lateral sensitivity is higher in the High mode. The inverted profiles (Fig. 4, right) reveal a two-layer structure with the interface set to 1 m depth. Conductivity values go from 5 to 65 mS/m. In profile 1, distinct metal boxes are clearly visible as conductive bodies at approximately 1 meter depth. An anomalous zone is also observed in the second profile between meters 5 and 10, where the low mode indicates a resistive body, while the High mode shows a conductive anomaly.

The quality of all inversions is considered satisfactory, since RMSPE value is around 10%, which is common for this kind of studies. These results were achieved after several trials and parameter adjustments, corresponding to the models with the lowest RMSPE values. The study allowed characterization of the subsurface down to approximately 2 meters depth.

## IV. DISCUSSION OF RESULTS

Since both profiles have a cut-off point, the correlation between them is analysed. In Figure 5, the profiles show a common contact area without abrupt changes in trends. In both profiles, two layers can be identified with an interface at the same depth and comparable electrical conductivity values. Furthermore, the comparison between the two types of measurements, profiles and maps, is coherent. For this analysis (Fig. 5), the deepest mapping, C3, in High mode was used, as it

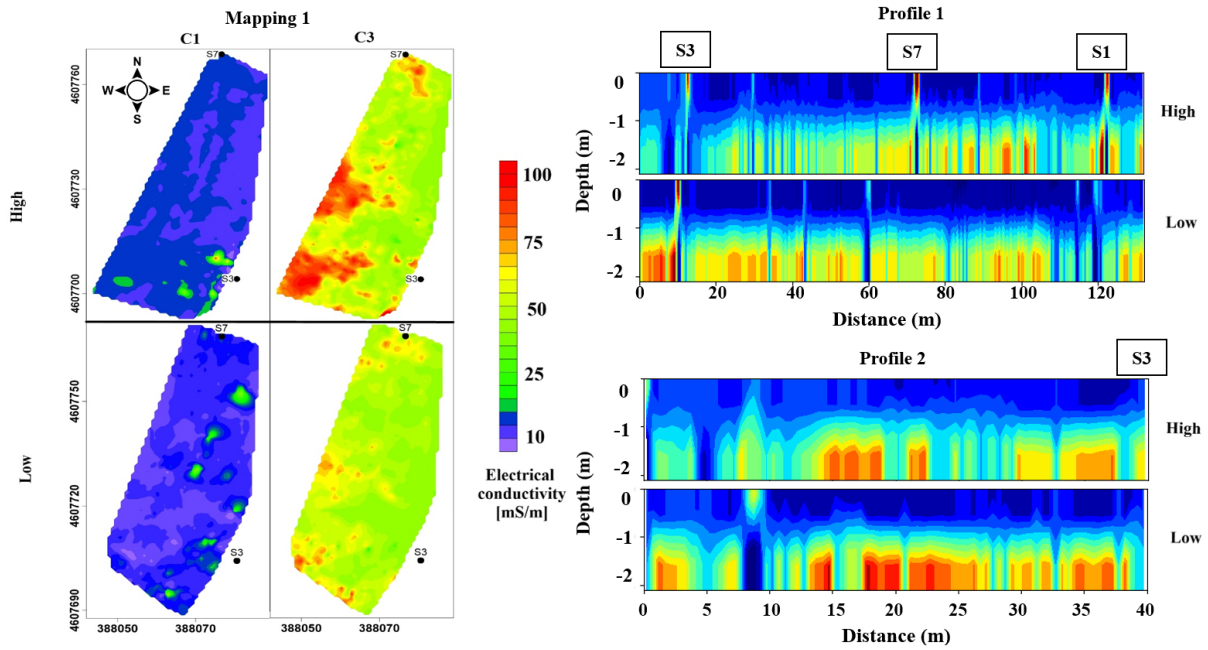


Figure 4: Inversion result for mapping 1 (C1 and C3) and the profiles in High and Low mode [6].

presents the greatest contrast in values and allows for a clearer identification of potential discrepancies or similarities between both measurement types. The red conductive areas are particularly suitable for evaluating

this correspondence, as they are clearly delimited in the maps and intersected by the profiles.

The comparison with lithological studies indicates a change in conductivity about one meter below the surface. The geological information indicates that the shallowest layer consists of gravel fill with clay and silt, extending from 0.8 to 1.2 meters deep, while the next layer of clay and silt with scattered gravel reaches up to two meters deep (CMD MiniExplorer sensibility limit), aligning with the identified conductivity layers. Sediment conductivity is affected by porosity, water content, and mineral composition of the fine fraction. Clays and silts exhibit higher conductivity due to their structure, which allows for a continuous conductive pore network. In contrast, gravels have a discontinuous clay matrix and lower conductivity [9]. These observations confirm that the most resistive layer is at the top. These properties are consistent with the order and values of the conductivity layers identified, in which the most resistive layer is located at the top.

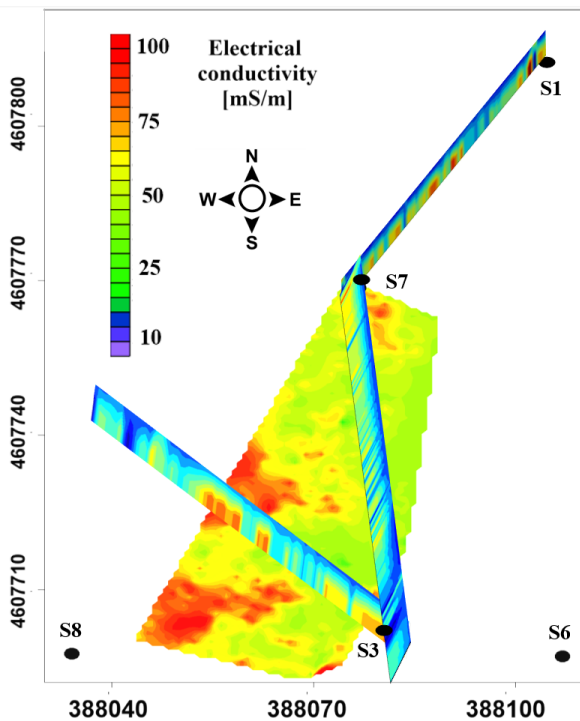


Figure 5: Comparison and superposition of the inverted profiles and Mapping 1 (C3), in High mode. [6]

The anomaly detected in the second profile, between meters 5 and 10, was also visible on the surface through a marked change in vegetation, with significantly taller grass in the anomalous zone (Fig. 6). The different interpretations of the anomaly depending on the mode of the CMD Mini Explorer are beyond the scope of this study - it would require additional measurements, alternative methods, and further expertise - but the strong inversion response indicates the presence of an anomalous body. Potential explanations include a recent

filling or the remains of a former pipe. Historical records indicate that a pipe carrying contaminated water to the reservoir previously crossed this area and was reportedly removed during earlier remediation works [1].



Figure 6: Picture during the work field where the tall grass anomaly is constatable.

However, no other anomalies are observed that we can attribute to the presence of contaminants. It is probable that DNAPL is no longer present within the first 2 m of the subsoil, having either migrated to greater depths or been eliminated. If DNAPL were still present, the expected anomaly would appear as resistive in its free phase (not dissolved in water) or conductive in solution (J. Luque Marín, personal communication: email, 6 June 2025) .

The method applied has proven effective for shallow geophysical exploration, offering a coherent characterization of the subsurface down to approximately two meters. The characterization is consistent with the known lithology and previously available information about the site. The results are comparable regardless of whether the data were processed as profiles or grids, confirming the internal consistency of the methodology. Additionally, the method was time-efficient, easy to apply, and economic. Data processing was intuitive and provided a useful overview of subsurface structures, which made its usefulness for rapid and practical field investigations. Nevertheless, the method did not reveal

any signs of contamination. This technique proves unreliable for investigating DNAPL contaminated areas with characteristics similar to those at the Òdena site.

## V. CONCLUSIONS

In this work, a contaminated area has been characterized by using electrical conductivity. Two different layers have been confirmed, the deepest one as the most conductive, which is consistent with the known lithology. Also, the different types of measurements, profiles and mappings, are coherent. Some anomalies have been detected but none related to contamination.

This technique has proven to be a practical and accurate tool, capable of providing a rapid overview of the superficial area and supporting various studies, but contamination was not observed. The results should be interpreted with caution, given the depth limitations and the use of a 1D inversion model, which may sometimes oversimplify complex subsurface conditions.

In future work, it would be of interest to study in detail some of the anomalies detected in order to determine their origin. In addition, since this technique is quite reliable, easy to implement, cost-effective, and fast, it could be particularly valuable for early-stage investigations of surface contamination during the initial phases of infiltration. The use of other techniques not so limited by depth would also be interesting.

## Acknowledgments

I would like to sincerely thank Dr. Pilar Neus Queralt and Dr. Alex Marcuello for their teachings, time, and support. I am also grateful to Dr. José Luque Marín and José Jiménez Guíñez for their assistance, data, and valuable insights. Lastly, I thank my brother and family for their continued support and review.

- 
- [1] D. Rodríguez-Fernández et al., “Unravelling long-term source removal effects and chlorinated methanes natural attenuation processes by C and Cl stable isotopic patterns at a complex field site,” *Sci. Total Environ.*, vol. 645, pp.286–296, 2018.
  - [2] GF Instruments, *CMD Electromagnetic Conductivity Meter User Manual V2.0*, Czech Republic. [No publication date stated].
  - [3] J. López Zancajo, *Viability of Detecting Fresh Water on the Coastline Using EM Methods*, Bachelor’s thesis, Facultad de Física, UB, Barcelona, Spain, Jun. 2024.
  - [4] GF Instruments, *Short guide for electromagnetic conductivity mapping and tomography*, Czech Republic, 2020.
  - [5] P. McLachlan, G. Blanchy, and A. Binley, “EMagPy: Open-source standalone software for processing, forward modeling and inversion of electromagnetic induction data,” *Comput. Geosci.*, vol. 142, Art. no. 104561, 2020, doi: 10.1016/j.cageo.2020.104561.
  - [6] G. Blanchy and P. McLachlan, “EMagPy python API and standalone GUI,” 2020. [Online]. Available: <https://hkex.gitlab.io/emagpy/#> [Accessed: 8-Jun-2025].
  - [7] GF Instruments, “Geophysical instruments,” [Online]. Available: <http://www.gfinstruments.cz/>. [Accessed: 8-Jun-2025].
  - [8] Google Earth Pro, version 7.3.6.10201, [Computer software], Google LLC, 2025
  - [9] A. Revil and P. W. J. Glover, “Nature of surface electrical conductivity in natural sands, sandstones, and clays,” *Geophys. Res. Lett.*, vol. 25, no. 5, pp. 691–694, Mar. 1998, doi: 10.1029/98GL00296.

## Aplicació de tècniques electromagnètiques a l'exploració del subsol

Author: Imma Gonzalez Prats

Facultat de Física, Universitat de Barcelona, Diagonal 645, 08028 Barcelona, Spain.

Advisor: Alejandro Marcuello Pascual, alex.marcuello@ub.edu

**Resum:** Aquest treball explora en profunditat les bases del mètode d'inducció electromagnètica i l'utilitza per caracteritzar la conductivitat elèctrica del sòl en una àrea contaminada prop d'Odena (Catalunya, Spain). L'objectiu del treball és avaluar la viabilitat del mètode. El procés consisteix en la recollida i anàlisi de dades de conductivitat aparent mitjançant el CMD Mini Explorer, la seva inversió amb el programa EMagPy i la seva representació gràfica amb el Surfer. Comparant les diferents mesures amb estudis disponibles de la zona és possible caracteritzar-la i identificar-hi de manera fiable anomalies i les seves tendències.

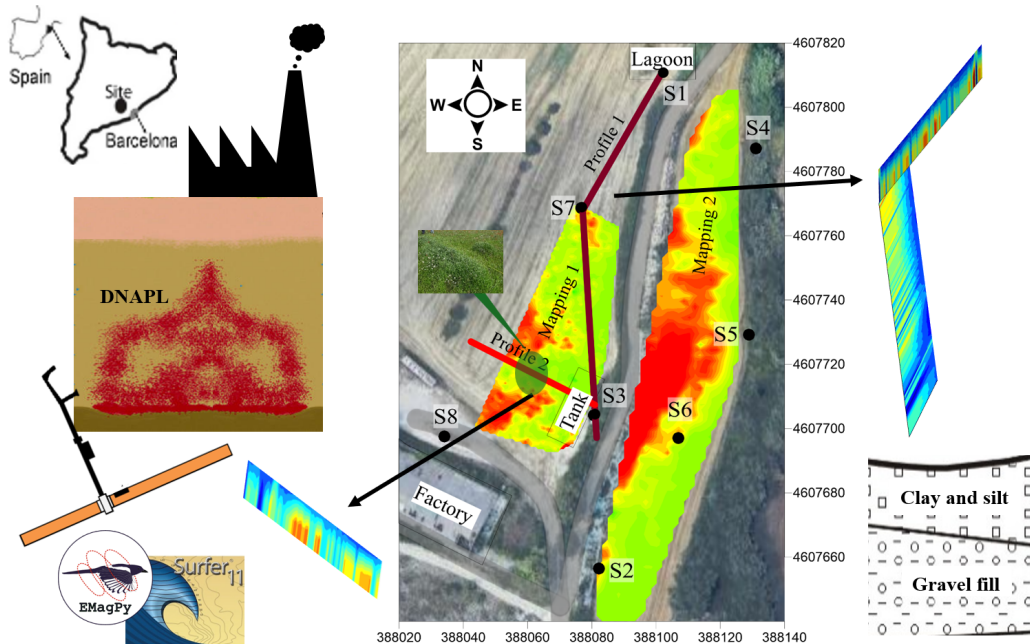
**Paraules clau:** conductivitat elèctrica, mètodes d'inducció electromagnètica, contaminació de sòls  
**ODSs:** salut i benestar (3), aigua neta i sanejament (6), vida de ecosistemes terrestres (15), aliances per aconseguir els objectius (17)

### Objectius de Desenvolupament Sostenible (ODSs o SDGs)

1. Fi de la es desigualtats		10. Reducció de les desigualtats	
2. Fam zero		11. Ciutats i comunitats sostenibles	
3. Salut i benestar	X	12. Consum i producció responsables	
4. Educació de qualitat		13. Acció climàtica	
5. Igualtat de gènere		14. Vida submarina	
6. Aigua neta i sanejament		15. Vida terrestre	X
7. Energia neta i sostenible	X	16. Pau, justícia i institucions sòlides	
8. Treball digne i creixement econòmic		17. Aliança pels objectius	X
9. Indústria, innovació, infraestructures			

Aquest Treball de Fi de Grau de Física està relacionat amb l'ODS 3, especialment la fita 3.9, ja que analitza un subsòl contaminat per químics perillosos per la salut. L'estudi pot ser útil per a l'anàlisi de la contaminació de l'aqüífer on drena el subsòl, vinculant-se amb la fita 6.3 de l'ODS 6 i amb la gestió sostenible dels ecosistemes del territori, relacionant-se amb la fita 15.1 de l'ODS 15. Finalment, per la interacció amb altres estudis i la dimensió global del tema, es relaciona amb l'ODS 17.

### GRAPHICAL ABSTRACT



## Appendix: Complementary information

## Studied area and field work pictures



FIG. A1: Mapping 1 (left) area and Mapping 2 area (right) pictures during the field work.

## RMPSE graphic

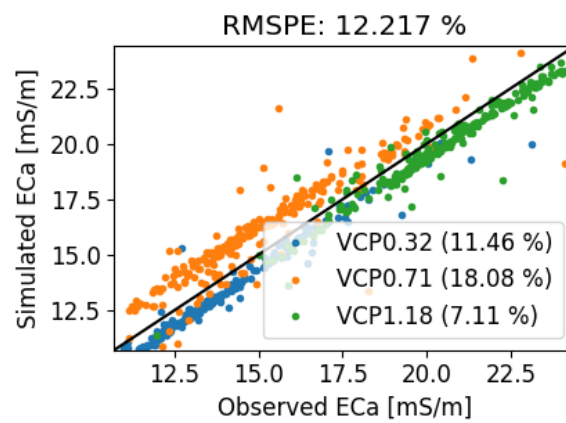


FIG. A2: Example of a RMSPE graphic (Profile 1 mode Low).

Completed real data mappings

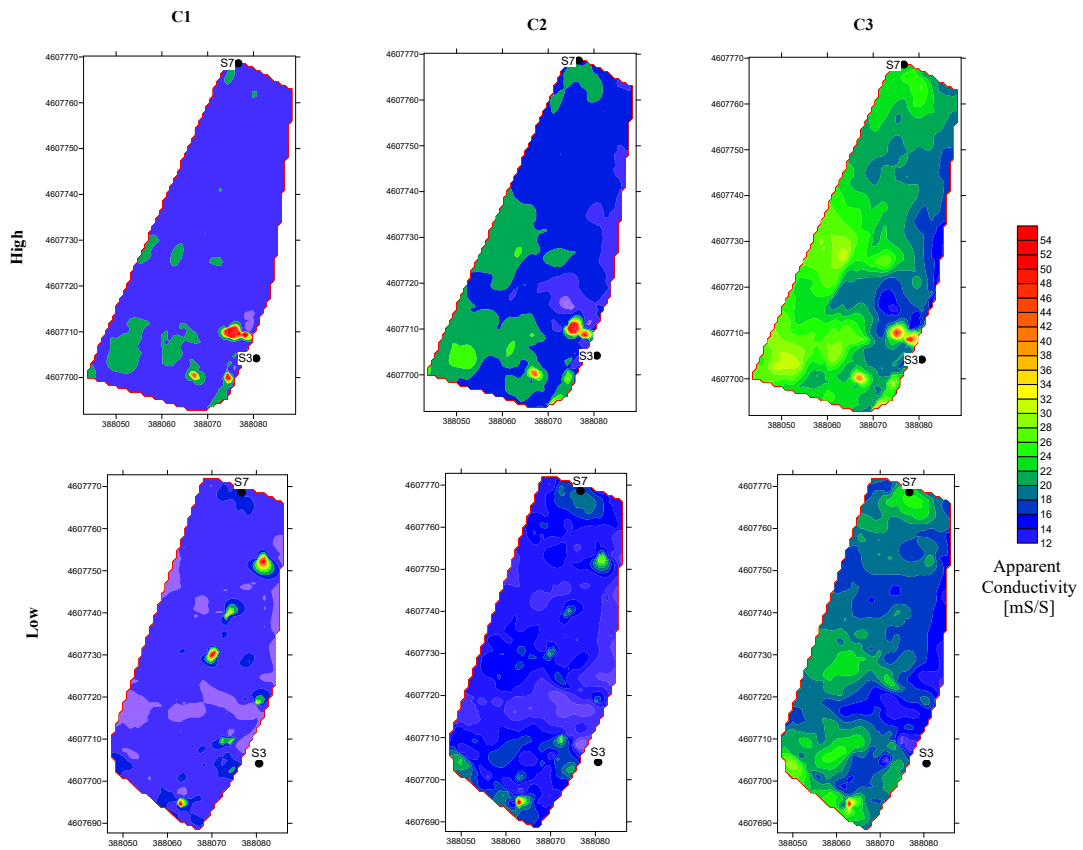


FIG. A3: Real data Mapping 1 with Surfer: High and Low mode (C1, C2 and C3)

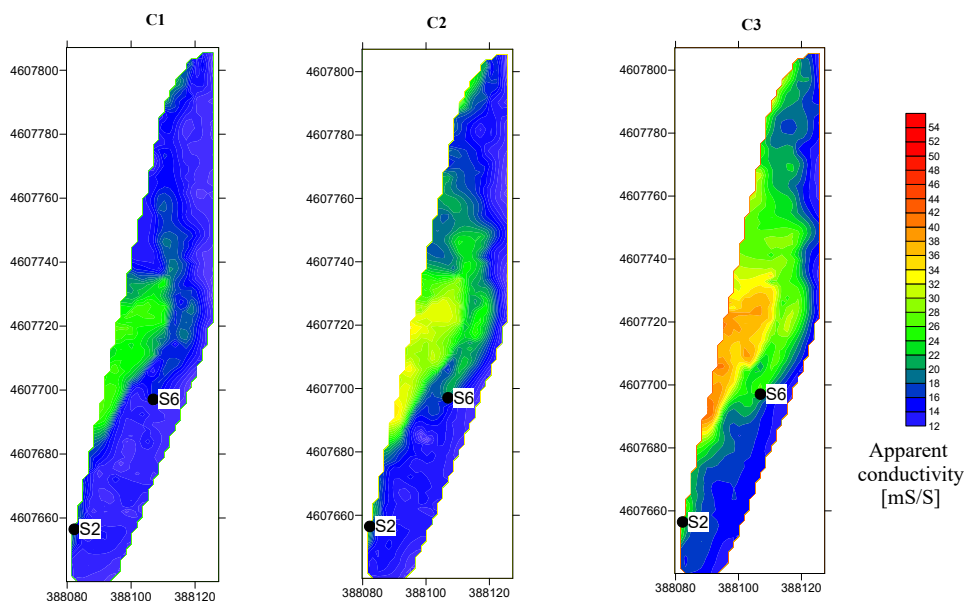


FIG. A4: Real data Mapping 2 with Surfer: High mode (C1, C2 and C3).

Completed inverted data mappings

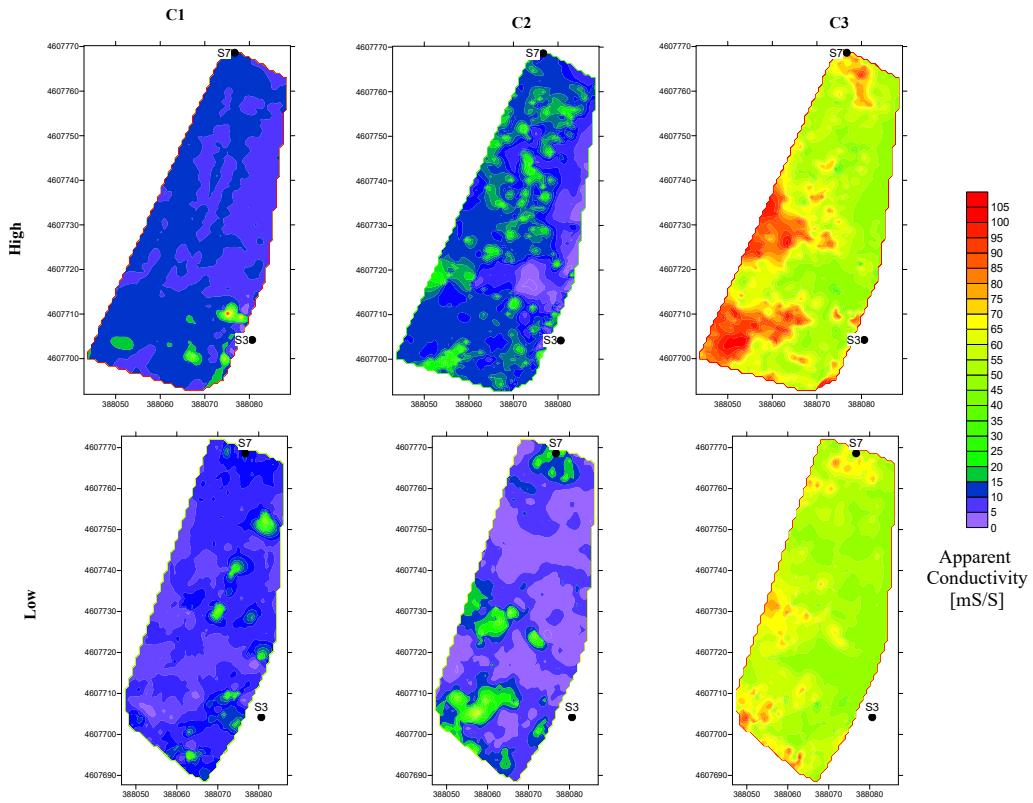


FIG. A5: Inverted data Mapping 1 with Surfer: High and Low mode (C1, C2 and C3)

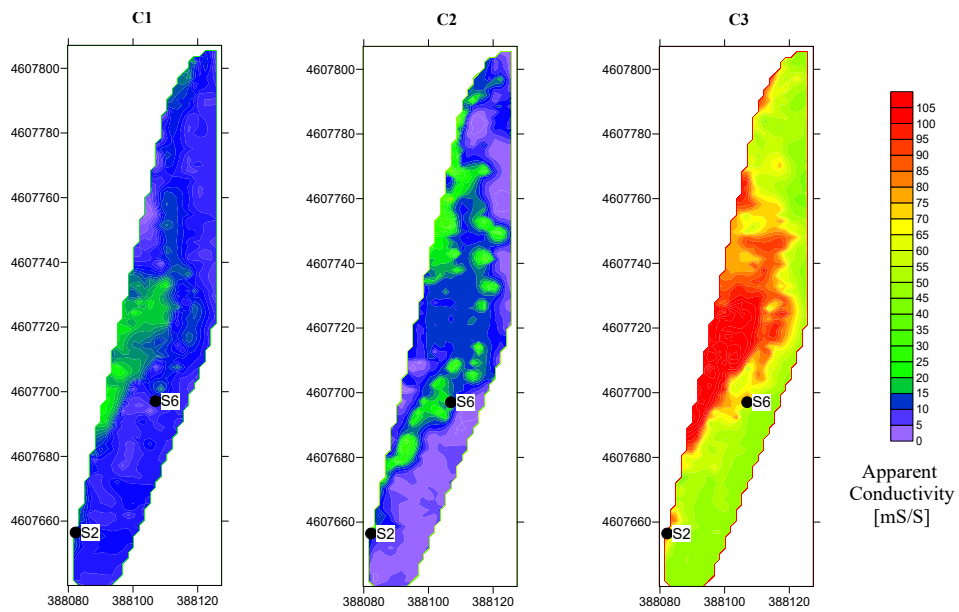


FIG. A6: Inverted data Mapping 2 with Surfer: High mode (C1, C2 and C3).